



# Sediment dynamics, neotectonic activity and palaeoenvironments recorded in the Quaternary infill of the central Upper Rhine Graben

Lukas Gegg<sup>a,\*</sup>, Olivier Moine<sup>b</sup>, Philipp Stojakowits<sup>c,d</sup>, Frank Preusser<sup>a</sup>

<sup>a</sup> Institute of Earth and Environmental Sciences, University of Freiburg, Albertstraße 23b, 79104, Freiburg, Germany

<sup>b</sup> Laboratoire de Géographie Physique, UMR 8591, CNRS-Université Paris 1-UEPEC, 2 rue Henri Dunant, 94320, Thiais, France

<sup>c</sup> Landesamt für Bergbau, Energie und Geologie (LBEG) and Bundesanstalt für Geowissenschaften und Rohstoffe (BGR), Stilleweg 2, 30655, Hannover, Germany

<sup>d</sup> Institute of Geography, University of Augsburg, Alter Postweg 118, 86159, Augsburg, Germany

## ARTICLE INFO

### Keywords:

Central Europe  
Chronostratigraphy  
Lithostratigraphy  
Luminescence dating  
Malacology  
Palynology  
Pleistocene

## ABSTRACT

The Upper Rhine Graben is a large-scale tectonic basin in central Europe that has accumulated a kilometre-thick sedimentary succession including, in some places, several hundred metres of mostly continuous Quaternary strata. Especially in the central graben part, these strata have hardly been scientifically explored. We introduce a new, 45-m-long drill core record from the vicinity of Offenburg. At its base, it comprises glaciofluvial gravels derived from the Alpine headwaters, which are superseded by aeolian deposits intercalated with locally derived gravels distinct by a different gravel spectrum. Post-infrared infrared-stimulated luminescence dating shows that the entire sequence reaches back beyond 300 ka, and that the glaciofluvial-aeolian transition occurred during the penultimate glaciation at ~160 ka. By comparison with neighbouring boreholes, we infer repeated normal faulting south of the drill site since roughly the same time, with the resulting topography filled in by locally sourced gravel interbeds. Finally, two layers of fines indicating stagnant palustrine conditions contain interstadial pollen assemblages of the penultimate and last glaciation, and shells of gastropods typical of Pleistocene loess deposits and a glacial palaeoclimate are encountered in the aeolian succession. Thus, this study offers insights into Middle to Late Pleistocene sediment dynamics, neotectonic activity and palaeoenvironments, and highlights the wealth of stratigraphic information that the Upper Rhine Graben preserves.

## 1. Introduction

The Upper Rhine Graben (URG, Fig. 1), part of the European Cenozoic Rift System (Ziegler, 1992), is a large-scale tectonic basin formed by extension and subsidence in response to the Alpine orogeny starting in the Palaeogene (e.g. Dèzes et al., 2004; Schumacher, 2002). The subsurface of the graben is intensively dissected by faults, with pronounced differential subsidence of the resulting blocks that is continuing until today. This is evidenced by instrumental data (e.g. Barth et al., 2015), severe historic earthquakes (e.g. Lambert et al., 2005), as well as surface deformation (e.g. Peters and Van Balen, 2007a; Pena-Castellnou et al., 2023). The long-lasting subsidence allowed for the accumulation of a kilometre-thick sedimentary sequence (GeORG-Projektteam, 2013) including, locally, several hundred metres of Quaternary deposits (Hagedorn and Boenigk, 2008; Gabriel et al., 2013, and references therein). This young infill of the URG is, due to its central position in Europe, its first-order continuity over many glacial cycles (although

hiati certainly exist, e.g. Gegg et al., 2024b), and its large source area, a scientific archive of supra-regional relevance (Gabriel et al., 2013). In the southern, proximal graben part it consists of a large-scale alluvial fan of gravel deposits derived from the Alpine headwaters of the Rhine system (Ellwanger, 2011; Ellwanger et al., 2011; Gegg et al., 2024a; Kock et al., 2009). These were episodically deposited by high-discharge events during peak glacial or incipient deglacial conditions, and are therefore an archive of the Alpine glaciation history. At the northern end of the URG, the sedimentary succession is significantly more complex. Here, notably in the graben's depocentre in the Heidelberg Basin (southeast of Mannheim, Fig. 1), fluvial, lacustrine, palustrine, and colluvial sediments occur that are much more variable in facies and provenance (Ellwanger et al., 2012; Gabriel et al., 2013, and references therein; Gegg et al., 2024b; Preusser et al., 2021; Scheidt et al., 2015).

In contrast, the correlative deposits in the central part of the URG are only poorly explored. These are referred to as Ortenau Formation (Fm.; formerly 'Unteres Kieslager' to 'Oberes Kieslager' sensu Bartz, 1982)

\* Corresponding author.

E-mail address: [lukas.gegg@geologie.uni-freiburg.de](mailto:lukas.gegg@geologie.uni-freiburg.de) (L. Gegg).

<https://doi.org/10.1016/j.qsa.2025.100284>

Received 30 January 2025; Received in revised form 24 April 2025; Accepted 1 May 2025

Available online 8 May 2025

2666-0334/© 2025 The Authors. Published by Elsevier Ltd. This is an open access article under the CC BY-NC license (<http://creativecommons.org/licenses/by-nc/4.0/>).

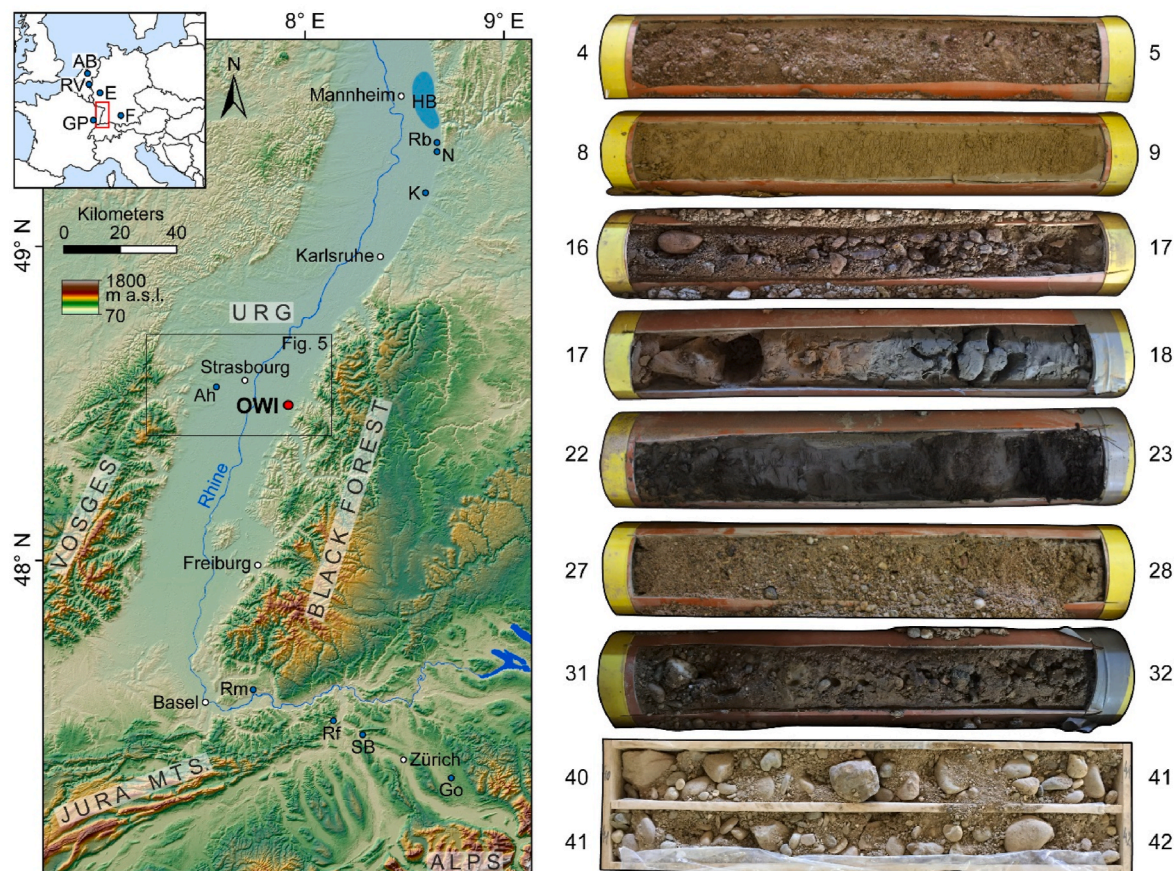


**Fig. 1.** Overview map of the Upper Rhine Graben (URG) with position of the OWI drilling at Offenburg (left; red dot), together with photographs of selected drill cores reflecting the sediments' variability (right; top and bottom depth in meters indicated). Marked in blue on the map are reference sites mentioned in the text: AB – Amersfoort Basin, Ah – Achenheim, E – Eifel, F – Füramoos, Go – Gossau, GP – Grand Pile, HB – Heidelberg Basin centre, K – Kronau, N – Nussloch, Rb – Rösbach, Rf – Rinikerfeld, Rm – Riedmatt, RV – Roer Valley Graben, SB – Sulzberg-Baden.

after the historical name of the region, and consist of undifferentiated sandy and, especially in the deeper part, silty gravels that become progressively finer towards the north, and intercalate with sandy-silty deposits (Ellwanger, 2011; Ellwanger et al., 2012; Wirsing and Luz, 2007). Their maximum thickness reaches values of more than 200 m in the graben centre but is generally variable and decreases toward either margin (GeORG-Projektteam, 2013). Chronostratigraphically, they represent presumably the entire Quaternary but time markers are scarce (Boenigk, 1987; Brost et al., 1991), and deposition, tectonically controlled, may have been discontinuous (cf. Gegg et al., 2024b). The material consists of a far-travelled component from the Alps as well as a local component, which is prominent especially near the graben shoulders (Wirsing and Luz, 2007). There, considerable deposits of loess, aeolian silt deflated, for example, from meltwater-fed braided riverbeds, occur as well (Antoine et al., 2009; Lehmkuhl et al., 2021; Schulze et al., 2022; Schwahn et al., 2023).

Previously, the URG has been explored mainly from an applied point of view focusing on, for example, its groundwater reservoirs (Wirsing and Luz, 2007), on geothermal energy production (GeORG-Projektteam, 2013), or on lithium extraction (Kölbel et al., 2023). This study targets the Quaternary depositional record in the central part of the graben as a stratigraphic archive and introduces the first drill core from this area to an international audience. The core has been recovered near the city of Offenburg, is 45 m long, and comprises all the above-mentioned depositional facies. It is investigated by a combined sedimentological approach integrating lithostratigraphic (facies and compositional analyses), geochronological (luminescence dating), and biostratigraphic

(palynology and malacology) methods. With this approach, we reconstruct sediment dynamics, neotectonic movements and palaeoenvironments in one of Europe's key areas for Quaternary stratigraphy (Gabriel et al., 2013) over a timespan of more than 300 kyr.

## 2. Material and methods

### 2.1. Core selection and recovery

The drilling at Offenburg-Windschläg (OWI; Fig. 1) is part of a S-N transect of exploration boreholes drilled for the planned expansion of the railway line along the Upper Rhine Plain. This specific core – archive number 7413/1476 of the State Geological Survey LGRB – was selected for further investigation based on a previous borehole log in close vicinity that registered organic-rich fines at ~137 m a.s.l. Drilling was conducted in 2022 some 4 km north of the city of Offenburg (48.5095° N, 7.9645° E) at ~159 m a.s.l., first in 1-m-length, 20-cm-diameter plastic liners (0–32 m depth), then without liners in a single-tube core barrel (32–45 m depth). Full recovery was reached, but 6 m of the core were withdrawn for analysis by the drilling contractor and were not available for this study (see Fig. 2). The in-liner section was generally of excellent core quality, whereas the sediments from the deeper part of the borehole, recovered without liners, were filled into core boxes, resulting in internal disturbance. The profile was described and sampled in interim storage at a core repository of the German Railway Service in Offenburg.

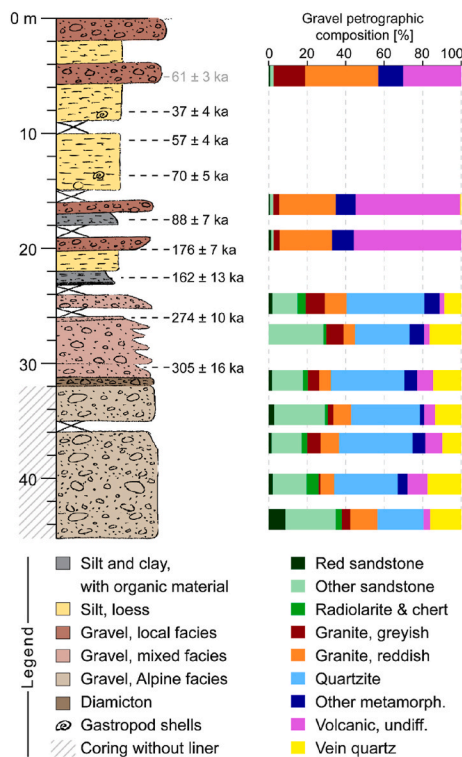


Fig. 2. Overview log of the OWI profile with luminescence ages (MET-pIRIR 200 °C) and petrographic composition of gravel samples. Gaps in the profile (X) mark core metres withdrawn by the drilling contractor.

## 2.2. Sampling and sedimentological analysis

Eight volumetric gravel samples taken between 5 and 44 m depth were sieved into cobble (>63 mm), coarse (63–20 mm) and medium gravel (20–6.3 mm), as well as a fine fraction (<6.3 mm), and grain size distribution curves were determined. The coarse gravel fractions, consisting in most cases of at least ~100 clasts, were further investigated for their gravel petrographic composition (cf. Gegg et al., 2024a). For luminescence dating, nine samples were taken in metal tubes pushed into the 20-cm-thick in-liner cores, and tightly sealed with opaque tape. The surrounding sediment was collected for gamma spectroscopy. Two intervals of fine-grained deposits at 17–18 and 22–23 m depth were sampled discontinuously at a 5-cm-resolution. There, carbonate and total organic carbon (TOC) contents were measured by the loss-on-ignition approach (Heiri et al., 2001) as outlined in Gegg et al. (2024b), and subsamples of few grams were saved for pollen extraction. Finally, at depths of 9 and 13 m, small (~1 mm) dispersed snail shells were encountered in cores from OWI and two neighbouring drillings, and bulk sediment samples of ~0.5 L each were taken for screening for gastropod fossils.

## 2.3. Luminescence dating

Preparation of the luminescence samples was done in the red-light laboratory at the University of Freiburg. Samples OWI-1, OWI-6, OWI-7 and OWI-8 were of sandy nature and therefore the coarse grain approach was used. Here, samples were sieved to 100–200 µm, carbonates were removed with 20 % HCl, and K-feldspar was separated from other minerals using a heavy liquid ( $\delta = 2.58 \text{ g cm}^{-3}$ ). K-feldspar grains were mounted on stainless steel discs with a diameter of 1 mm coated with silicon oil as adhesive. For the other samples, the fine grain technique was applied. Here, the sample material was subsequently treated with 20 % HCl, 30 % H<sub>2</sub>O<sub>2</sub> and Na-oxalate to remove carbonate, oxidise organic matter and disperse clay minerals, respectively. Each

step was followed by rinsing the sample five times with demineralised water. The fraction 4–11 µm was enriched by settling in water using Stokes' Law (cf. Frechen et al., 1996), dried, and then pipetted on stainless steel discs for measurements. Previous studies have shown that quartz from this part of the URG usually has poor signal properties (i.e. overall low signal intensity and different behaviours of natural and artificially irradiated signals; Lauer et al., 2010; Preusser et al., 2016, 2021). Furthermore, it was expected that the sequence will reach beyond the dating limits of quartz. Hence, in this study we rely on feldspar as natural dosimeter, which has proven reliable in previous studies (e.g. Preusser et al., 2016, 2021; Marik et al., 2024).

Luminescence measurements were carried out on a Freiberg Instruments Lexsyg Standard device (Richter et al., 2013). To narrow the transmission window to the main luminescence emission of K-feldspar (410 nm), a 3-mm-thick Schott BG 39 glass filter in combination with a 414/46 AHF Brightline interference filter was used. The beta source in the machine was calibrated using the LexCal2014 quartz (Richter et al., 2020) to ca.  $0.12 \text{ Gy s}^{-1}$  on stainless steel discs. For determination of the equivalent dose ( $D_e$ ), a modified version of the Single Aliquot Regenerative (SAR) dose Multi-Elevated Temperature (MET) post-infrared stimulated (pIRIR) luminescence protocol with five irradiation cycles including zero dose and recycling was used, applying a preheat at 270 °C for 60 s (Li and Li, 2011). The stability of the signal increases with stimulation temperature, and therefore the effect of fading (i.e. signal loss) that leads to the underestimation of feldspar signals – if not corrected for – can be eliminated. Li and Li (2011) report stable signals not affected by fading for stimulation temperatures of 200 °C and 250 °C. Fitting of growth curves was done using the sum of two exponential functions, which provided a much better fit than using a single exponential function. For the coarse-grained samples, mean  $D_e$  was determined for 12 replicate measurements, while for the fine-grained samples the number of replicate measurements was limited to seven considering the excellent reproducibility.

For dose rate calculation, the concentration of relevant elements (K, Th, U) was determined by gamma spectroscopy. Samples were dried, water contents determined, and the material was filled into plastic containers and measured using an Ortec High Purity Germanium gamma spectrometer (details in Preusser et al., 2023). For dose rate determination we used the ADELEV2017 software (Degering and Degering, 2020; www.add-ideas.com, last accessed Nov 24th 2024), assuming an alpha efficiency of  $0.07 \pm 0.02$ . The average water content was estimated based on the measured values adding an error margin of 20 % to account for uncertainty.

## 2.4. Pollen and gastropod identification

Extraction and identification of pollen and macrofossils follows Faegri and Iversen (1989). For pollen extraction, samples were pre-treated with 10 % HCl, then spiked with *Lycopodium* spores and cooked in 10 % KOH. The pollen grains were isolated by density separation, acetolysed, and fixed in glycerine. Specimens were identified at 400x and 1000x magnification with regard to the pollen key of Beug (2004) as well as a reference collection. Below 22 m depth, pollen percentages were calculated from sums of  $\geq 600$  terrestrial pollen grains. Above 18 m depth, the majority of the samples was counted to  $\geq 600$  arboreal pollen grains resulting in reference sums of more than 1000 terrestrial pollen grains. Reference sums were calculated excluding Cyperaceae, aquatics and spores. Pollen and spore nomenclature follows Beug (2004) and Reille (1998), respectively.

Bulk sediment samples containing gastropod shells were wet-sieved using several mesh sizes from 8 to 0.25 mm, and macrofossils collected with a needle and a fine wet brush. The specimens were identified under a binocular microscope using the European atlas of Welter-Schultes (2012) and reference collections, named according to the international mollusca base (Bank et al., 2014; www.molluscabase.org, last accessed Jan 10th 2025), and species distributed in ecological

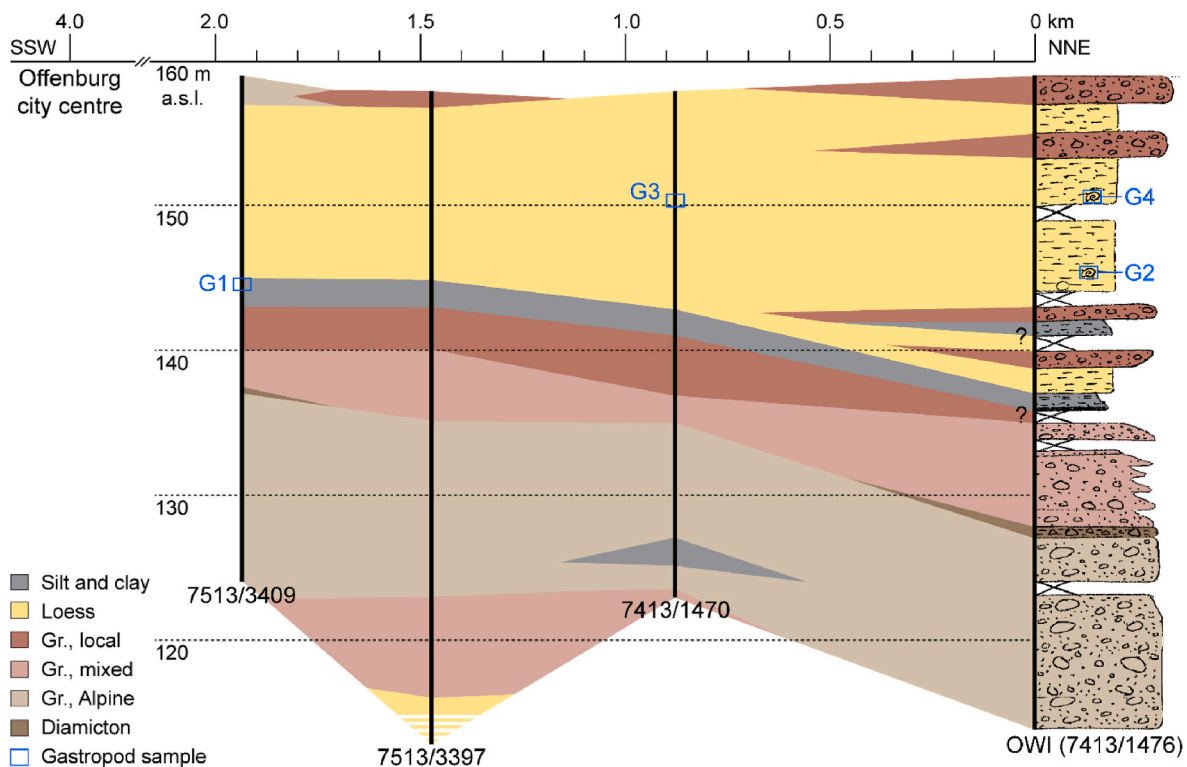


Fig. 3. Neighbouring boreholes to SSW of OWI recovered generally similar successions, but with differences in the depth of layer boundaries. At lower stratigraphic levels, mixed-facies gravels and loess, partly reworked (hatched white), occur. Gx mark samples collected for gastropod extraction and identification (see Table 2).

groups defined by Ložek (1964), Puisségur (1976), and Rähle (2005).

### 3. Results

#### 3.1. Sediment sequence

The bottom half of OWI, from ~23 to 45 m depth, comprises beige-grey, fines-rich, sandy gravel (Figs. 1 and 2). The individual clasts are well-rounded and consist mainly of quartzite, vein quartz and sandstones (Fig. 2). Below 32 m,  $D_{50}$  (i.e. median grain sizes) range between 12 and 17 mm, and  $D_{90}$  between 50 and 90 mm. From 31.3 to 32.0 m, a diamictic interbed contains subrounded clasts in a yellowish, partly brownish to reddish, matrix. Above, the gravel appears generally finer and consists of several fining upwards-cycles. Sporadically, admixtures of reddish, angular coarse sand to fine gravel can be identified. Coaly plant fragments occur within a massive bed of grey fine to medium sand at 26.0–26.3 m.

A layer of blackish, organic-rich (~10 % TOC, frequent cm-sized plant fragments) silt and clay at 23.0–22.6 m transitions into dark grey, silty-sandy clay with only little, smaller plant fragments, ~3 % TOC, and muscovite flakes (22.6–22.0 m; Fig. 1). Further up, these fines turn light bluish-grey with iron oxide precipitates and irregular, gravel-sized concretions (22.0–21.7 m) and then, gradually, ochre-beige (21.7–21.1 m). This last interval is faintly laminated and contains few outsized clasts at 21.4 and 21.2 m. Macroscopic organic material is lacking. A layer of very poorly sorted reddish sand from 21.1 to 21.0 m might be caving material fallen into the drilling tube from above. It is overlain by patchy reddish to ochre-beige silty clay up to 20.2 m.

At 20.2–19.0 m, a gravel bed is intercalated that is grey at its base but becomes more and more reddish upward. This red gravel type differs strikingly from the beige-grey gravel below. It is notably finer ( $D_{50} < 6.3$  mm,  $D_{90}$  between 30 and 40 mm) and consists of frequently angular clasts of crystalline rocks, predominantly purple volcanics and reddish granites (Fig. 2). Separated by another interval of clayey and sandy silt

with plant fragments and ~1 % TOC, changing in colour from bluish grey to ochre-red, a second red gravel bed occurs at 16.0–17.0 m. The remainder of the profile consists mainly of massive or faintly layered (mm-to cm-scale) ochre-beige silt with little fine sand. From 14.3 to 15.0 m depth, the silt has a prominent reddish hue and contains outsized clasts up to gravel size, and at 8–9 and 13–14 m, it contains dispersed small coaly plant fragments and gastropod shells (see below). Two more interbeds of sandy red gravel occur at 5.9–3.9 and 2.0–0 m depth.

Three southward-adjacent boreholes that together with OWI span a 2-km-long transect show similar stratigraphic successions (Fig. 3). All of them recovered mostly grey gravels in their lower halves separated by red or mixed-facies gravels and organic-rich fines from dominantly orange-beige silts, but there are some differences a well. The layer boundaries are relatively shifted upwards by ~10 m towards the SSW. Red gravel intercalations in the upper part of the sequence occur only in OWI. Borehole 7513/3397 reached again mixed-facies gravels and, finally, another interval of orange-beige silt at its base (Fig. 3). Gastropod shells were encountered in two further boreholes located one (7413/1470) and 2 km to the south (7513/3409) at similar depth levels as in OWI.

#### 3.2. Luminescence ages

The results of luminescence dating are summarised in Table 1. Performance tests on the applied protocol resulted in dose recovery ratios within 10 % of unity and negligible thermal transfer. The MET protocol produces five estimates of  $D_e$ , which reflect the amount of radiation absorbed since the time of burial. For most samples, the  $D_e$  determined increases with stimulation temperature reflecting the fact that the pIR signal stimulated at higher temperatures becomes continuously more stable (cf. Li and Li, 2011). For several samples, the  $D_e$  determined for stimulation temperatures of 200 °C and 250 °C overlap within uncertainties, but the latter shows a lower saturation dose and performs less well in dose recovery tests. Following Schwahn et al. (2023), we

**Table 1**

Summary data of samples and the respective grain sizes used for pIR luminescence dating. Provided are water contents (WC), concentrations of dose-rate relevant elements (K, Th, U), the resulting dose rates (D), as well as  $D_e$  determined for different stimulation temperatures. The resulting pIR ages are based on the stimulation at 200 °C.

Sample	Depth (m)	Grain size (µm)	WC (%)	K (%)	Th (ppm)	U (ppm)	D (Gy ka <sup>-1</sup> )	$D_e$ IR-50 (Gy)	$D_e$ pIR-100 (Gy)	$D_e$ pIR-150 (Gy)	$D_e$ pIR-200 (Gy)	$D_e$ pIR-250 (Gy)	Age pIR-200 (ka)
OWI-8	5.4	100–200	16.4	2.50 ± 0.10	13.61 ± 0.67	3.39 ± 0.09	4.31 ± 0.19	114.6 ± 5.1	189.0 ± 8.4	229.2 ± 8.6	263.1 ± 9.8	273.3 ± 9.0	61 ± 3
OWI-4	8.2	4–11	21.6	1.28 ± 0.03	11.92 ± 0.74	3.65 ± 0.17	3.45 ± 0.34	118.3 ± 4.8	117.2 ± 2.9	121.5 ± 5.5	126.2 ± 8.2	133.8 ± 6.3	37 ± 4
OWI-9	10.7	4–11	20.5	1.30 ± 0.04	10.45 ± 0.60	3.03 ± 0.19	3.13 ± 0.23	137.1 ± 2.3	145.8 ± 3.1	168.0 ± 3.7	177.1 ± 3.7	184.8 ± 6.3	57 ± 4
OWI-5	13.8	4–11	25.0	1.87 ± 0.05	16.00 ± 0.89	4.05 ± 0.19	4.27 ± 0.31	197.1 ± 5.2	238.7 ± 4.6	270.8 ± 4.0	297.4 ± 4.9	284.7 ± 9.4	70 ± 5
OWI-10	17.8	4–11	24.2	2.16 ± 0.06	23.20 ± 1.22	5.42 ± 0.25	5.61 ± 0.45	231.2 ± 4.7	373.3 ± 10.0	444.2 ± 12.0	493.3 ± 15.2	549.5 ± 21.9	88 ± 7
OWI-1	20.1	100–200	17.4	2.04 ± 0.05	8.71 ± 0.56	2.38 ± 0.13	3.29 ± 0.13	288.8 ± 8.1	386.6 ± 15.8	511.7 ± 18.4	579.0 ± 20.4	667.9 ± 20.8	176 ± 7
OWI-3	22.7	4–11	47.5	1.44 ± 0.04	10.75 ± 0.67	4.02 ± 0.26	2.82 ± 0.25	304.6 ± 6.5	347.8 ± 8.4	407.7 ± 9.5	458.1 ± 16.0	446.1 ± 23.7	162 ± 13
OWI-6	26.2	100–200	29.0	1.94 ± 0.05	8.22 ± 0.42	1.83 ± 0.10	2.78 ± 0.13	341.7 ± 10.9	570.9 ± 19.5	711.6 ± 20.9	762.9 ± 21.6	827.7 ± 30.8	274 ± 10
OWI-7	30.2	100–200	20.9	1.78 ± 0.05	7.65 ± 0.52	1.84 ± 0.11	2.80 ± 0.16	341.2 ± 15.8	616.0 ± 24.2	782.6 ± 37.7	854.1 ± 39.5	938.7 ± 47.1	305 ± 16

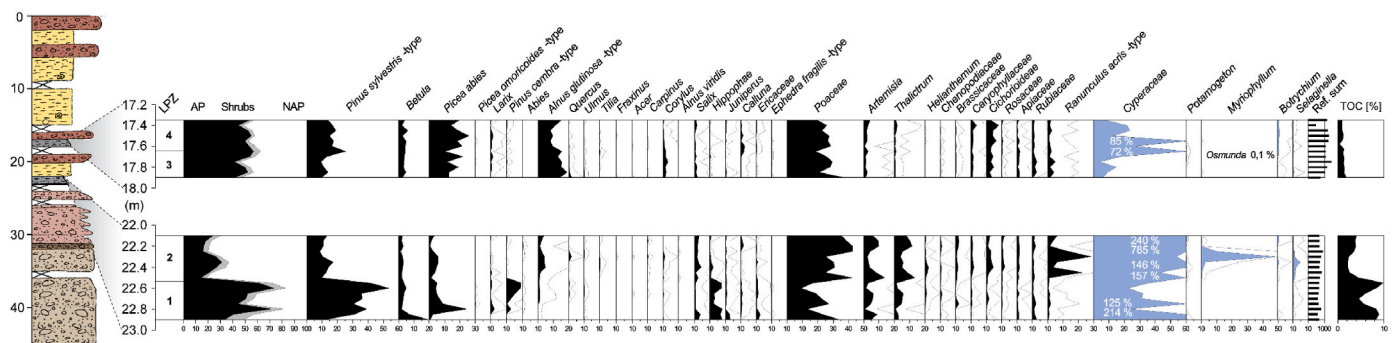


**Fig. 4.** Pollen diagrams from two selected intervals of the OWI record. Aquatic taxa are depicted in blue, and percentages refer to the respective sample's reference sum.

therefore regard the pIR signal stimulated at 200 °C as more reliable and focus on it in the discussion. However, the difference to ages calculated using the  $D_e$  of the signal stimulated at 250 °C differs by  $\leq 10\%$  of the mean and is mainly within uncertainties. With the exception of the topmost sample, ages increase with depth or overlap within uncertainties.

### 3.3. Pollen and gastropod content

Two intervals, from 22.9 to 22.1 m and from 17.9 to 17.3 m depth, were investigated for pollen contents at a 5-cm-resolution (Fig. 4). The local pollen zone 1 (LPZ 1; 22.9–22.5 m) is characterised by relatively high arboreal percentages (AP;  $>50$  up to 80 %), comprising *Pinus sylvestris*-type accompanied by *Picea*, *Pinus cembra*-type, *Hippophaë*, *Larix*, and *Betula*. Besides that, many heliophilous herbs occur, such as Poaceae, *Artemisia*, and *Thalictrum* as well as Cyperaceae, which were excluded from the pollen sum. LPZ 2 (22.5–22.1 m) shows around 20 % of arboreal taxa. The non-arboreal pollen (NAP) spectrum is dominated by Poaceae, and other heliophytes occur more frequently (e.g. *Artemisia*, *Thalictrum*, and *Ranunculus acris*-type) as well as further taxa typical for open conditions, like *Selaginella* and *Botrychium*. In LPZ 3 (17.9–17.7 m), Poaceae are prevalent and accompanied by *Alnus glutinosa*-type and *Picea*. *Pinus* is gaining subdominance in some samples. LPZ 4 (17.7–17.3 m) is also characterised by Poaceae dominance in most of the samples. Compared to the previous pollen zone, *Alnus* is less important but *Picea* and *Pinus* are more frequent.

In two horizons, gastropod shells were encountered during core description, and bulk sediment samples were collected for their extraction and identification (sample G2: 13.32–13.45 m, G4: 8.73–8.78 m depth). In two neighbouring boreholes, shells occurred at comparable depth levels, and two further samples were taken (G1 and G3,

respectively; Fig. 3). Between 12 and 37 specimens, belonging to ten terrestrial and one aquatic taxa mostly from mesophilous and open-land ecological groups, were found (Table 2).

## 4. Discussion

### 4.1. Depositional phases

The Quaternary succession recovered at OWI can be subdivided into two main depositional phases. These document a switch from dominantly (glacio-)fluvial deposition by the Rhine River to dominantly aeolian deposition, interrupted by some (locally sourced) fluvial and palustrine intercalations.

#### 4.1.1. Glaciofluvial phase

The lower part of the sediment sequence (~23–45 m depth) consists of well-rounded beige-grey sandy gravel (Figs. 1 and 2). This is the common facies of the Alpine-derived glaciofluvial outwash that represents the vast majority of the Quaternary infill of the southern URG (Ellwanger et al., 2011; Gegg et al., 2024a; Hagedorn and Boenigk, 2008). This gravel builds up a giant alluvial fan that can be traced far toward the distal graben end (Gabriel et al., 2013, and references therein; Preusser et al., 2021; Gegg et al., 2024b). A diamictic layer of unclear origin at ~32 m depth separates the glaciofluvial deposits into a coarser lower, and a finer upper gravel unit. The latter contains some locally derived material (reddish coarse sand and fine gravel; see below). In the coarse gravel fraction, the petrographic spectrum consists predominantly of quartzites, vein quartz clasts, and sandstones, which are typical lithologies of Alpine-derived glaciofluvial gravels (Gegg et al., 2024a, 2024b; Hoselmann, 2009; Preusser et al., 2021). This applies to the entire lower section, the two gravel units (32–45 and 23–31

**Table 2**

Gastropod findings from OWI and neighbouring drillings (cf. Fig. 3). \* Typical glacial taxa nowadays mostly living between 1000 and 3000 m a.s.l. in the Alps and Scandinavia (Welter-Schultes, 2012).

Ecological group	Species	G1	G2	G3	G4
Half-forested (mesophilous)	<i>Vitrea crystallina</i>	1	3		
Half-forested (humid and warm)	<i>Arianta arbustorum</i>	1		1	
Open land	<i>Columella columella</i> *	1		1	
	<i>Vallonia costata</i>	1	4		
Mesophilous	Slugs		3		
	<i>Trochulus hispidus</i>	19	20	8	1
Mesophilous (hygrophilous)	<i>Cochlicopa lubrica</i>		2		
Hygrophilous	<i>Succinella oblonga</i>	1		2	15
Palustral	<i>Pupilla alpicola</i> *		5		1
	<i>Vertigo genesii</i> *	2			
Aquatic (standing waters)	cf. <i>Stagnicola palustris</i>	1			
Earthworm granules		2		2	

m depth) cannot be differentiated based on gravel petrographic compositions. Interestingly, limestones and other carbonaceous lithologies, the main primary component of the Alpine meltwater gravels (Gegg et al., 2024a; Graf, 2009), are completely missing. We suggest that these have been dissolved after deposition due to specific local hydro-chemical conditions, as carbonate lithologies are still a large component of similarly aged gravels in other parts of the URG (Gegg et al., 2024b; Hoselmann, 2009). The beige fines within the gravels at OWI are thus interpreted, at least in part, as dissolution residues.

Two luminescence ages of ~300 ka place the upper glaciofluvial unit (23–32 m) into marine isotope stage 8 (MIS 8; after Lisiecki and Raymo, 2005), a global cold stage during which the Alpine headwaters of the Rhine catchment were glaciated (Preusser et al., 2011; Schlüchter et al., 2021). Presumed correlative deposits occur both upstream in the Alpine foreland (although their age determination is challenging; Graf, 2009; Claude et al., 2017; Buechi et al., 2018, 2024), as well as >100 km to the north at Kronau (Preusser et al., 2021) and in the Heidelberg Basin (Gegg et al., 2024b; Hoselmann, 2009). The lower gravel unit at OWI (32–45 m) was not suitable for dating due to a different drilling technique employed but might represent an older glaciation such as MIS 10 (~350 ka) or MIS 12 (~430 ka). Especially the latter could be a fitting candidate, as it is interpreted as the most extensive glaciation of the Alps (Preusser et al., 2011, 2021). Its large ice extent would have resulted in a comparatively short glaciofluvial transport distance towards the drill site, and probably in high sediment yields. This could explain the coarse, purely Alpine-derived gravel facies observed at 32–45 m depth. Evidence from two neighbouring boreholes (7413/1740 and 7513/3397; Fig. 3) suggests that older mixed-facies gravels and fines, as representative of the upper section of OWI (see below), are to be expected directly underneath, supporting the event-bed character of the interval (Ellwanger et al., 2011; Preusser et al., 2021).

#### 4.1.2. Aeolian phase

At a depth of ~23 m, the sedimentary facies and depositional setting change drastically (Fig. 2). The coarse-grained glaciofluvial outwash is replaced by predominantly ochre-beige silt that is interpreted as loess, fine material deflated from proglacial outwash plains and braided riverbeds and redeposited at the margins of the URG (Antoine et al., 2009; Lehmkuhl et al., 2021; Schulze et al., 2022; Schwahn et al., 2023). Luminescence ages suggest that loess deposition at the OWI site occurred in at least two stages during the penultimate (MIS 6) and the last glaciation (MIS 4 to 3). Major reworking of these aeolian sediments can probably be excluded, at least where well-preserved gastropod shells occur (Table 2). The loess sequence at OWI is interrupted by distinct interbeds of reddish, angular gravel composed mainly of red granitoids and volcanic rocks – lithologies that crop out east of the drill site in the northern Black Forest (LGRB, 2023). Therefore, these gravels represent events of intensive erosion and deposition after short-distance transport from the adjacent URG shoulder, likely also under periglacial conditions

(Ellwanger et al., 2009; Gegg et al., 2024b; Hoselmann, 2009). For sample OWI-8 (5.4 m depth), collected from these locally sourced gravels, the calculated luminescence age lies out of stratigraphic order and is higher than expected by a factor of ~2. The most likely explanation for age overestimation would be incomplete bleaching of the luminescence signal, although this sample does not show an increased scatter of  $D_e$  values (Murray et al., 1995). The observed overdispersion of the IR-50 signal of sample OWI-8 is 15 %, similar to values reported for nearby Late Pleistocene sites (Marik et al., 2024; Preusser et al., 2021). Since the dated layer is of local origin, we speculate it represents a high-energy event (such as a flash flood) during which little if any light exposure occurred. While it would have been worthwhile to cross-check the luminescence chronology, radiocarbon dating of the encountered gastropod shells was not considered as shell material from loess as old as ~40 ka has been reported as problematic in this context (e.g. Pigati et al., 2013).

#### 4.2. Neotectonic activity

A comparison with neighbouring boreholes reveals that locally sourced gravel interbeds are missing further to the SSW, and that they coincide in OWI with almost 10 m lower-lying stratigraphic boundaries in the basal part of the profile (Fig. 3). This can be explained by continued but episodic (post-MIS 8) differential subsidence of a fault-bound block below the drill site (cf. Fig. 4 in Stober et al., 2023) that on local scale created accommodation space for deposition of these gravels. This would require an average vertical slip rate of ~0.05 mm/yr, which is in the range of previous estimates from the URG (e.g. Peters and Van Balen, 2007a; Pena-Castellnou et al., 2023, and references therein). In fact, there are several documented cases of surface-rupturing (i.e. scarp-producing) palaeo-earthquakes in the URG (Nivière et al., 2008; Pena-Castellnou et al., 2023, 2025; Peters and Van Balen, 2007a; Shipton et al., 2017; Simon and Seyfried, 2020). Only ~30 km to the west, at Achenheim, France, at the opposite margin of the URG, Lemeille et al. (1999) reported a major active fault with a cumulated vertical offset of ~6 m since ~200 ka (dated by thermoluminescence; Buraczynski and Butrym, 1984), similar to what is observed at OWI (Fig. 5). Here, the thickness of the local-facies gravel interbeds of 1–2 m provides an estimate for the maximum displacement per event. A displacement of this order corresponds to an earthquake magnitude of 6–6.5 (Lemeille et al., 1999; Pena-Castellnou et al., 2023; Shipton et al., 2017), which is equal to that of the largest historic earthquake in the region (1356 AD at Basel; Lambert et al., 2005), and compatible with liquefaction attributed to ground shaking as reported nearby by

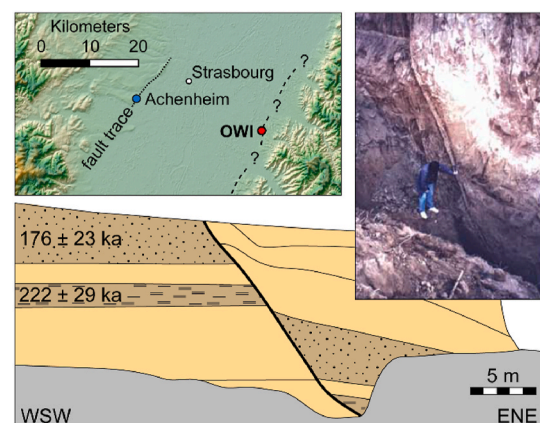


**Fig. 5.** The normal fault at Achenheim accumulated ~6 m of vertical displacement since ~200 ka, similar to the situation at OWI (sketch redrawn after Lemeille et al., 1999, thermoluminescence ages from Buraczynski and Butrym, 1984, photo from Bellier et al., 2021). Here, a potential fault scarp, less distinct than on the western graben side, can be identified as well (dashed line).

Montenat et al. (2007).

A second phenomenon that may be of tectonic origin is the drastic and permanent shift from glaciofluvial-dominated to aeolian-dominated deposition observed at OWI. This shift coincides roughly with the onset of neotectonic activity in the vicinity of the drill site as proposed above, and we consider it unlikely that it is a result of the depositional system's autocyclicality, i.e. the shifting of channel patterns due to sedimentary dynamics (Gegg et al., 2024b; Menzies and Ellwanger, 2015), alone. It is conceivable that larger-scale tectonic movements, for example subsidence in the graben centre, could have triggered a general westward shift of the Rhine course by relative lowering of the local base level. Interestingly, the opposite trend has been observed further to the north, in the Heidelberg Basin (Weidenfeller and Kärcher, 2008; Weidenfeller and Knipping, 2009). This is not implausible considering the fault-bound block nature of the URG basement, in particular in vicinity to its boundary fault systems (Peters and Van Balen, 2007a, 2007b; Shipton et al., 2017; Simon and Seyfried, 2020). However, the situation at OWI is more complex as the aeolian phase here begins after an interval of dark greyish fines (23–22 m depth) that are rich in plant fragments and contain aquatic taxa (especially *Myriophyllum*, LPZ 2). These fines point towards a period where subsurface conditions were stagnant and reducing, potentially in a palustrine environment (cf. Gegg et al., 2024b), which would imply, in contrast, a short-lived relative elevation of the local base level. These considerations suggest that repeated differential subsidence, and potentially relative uplift (Lang et al., 2011), of different-sized blocks can lead to complex depositional dynamics on a local to regional scale.

#### 4.3. Palaeoenvironment and biostratigraphy

Within the above-mentioned fines, the pollen assemblages of LPZ 1 (22.9–22.5 m) represent a succession from open (shrub) birch stands with juniper, willow, and buckthorn to an open forest mainly composed of pine and spruce, and later of *Pinus cembra*. This reflects the early, climatic optimum, and late stages of an interstadial (IS). The assemblages do not allow a palynostratigraphic classification on their own, but the luminescence data place the succession into MIS 6. Bludau et al. (1994) found an IS pollen sequence at Riedmatt at the upstream High Rhine (Fig. 1) within clays with a locally intercalated peat layer underneath glaciofluvial 'Hochtterasse' gravels of the penultimate glaciation. The three pollen profiles show some similarities to our record including dominance by *Pinus* and *Picea* (Bludau et al., 1994) that also occur in the lower part of the early MIS 6 Rinikerfeld record nearby (Gegg et al., 2023). The detected IS of LPZ 1 had a cool character resembling shortly and mildly ameliorated conditions. Such environmental conditions are known from (middle) Late Pleistocene IS as encountered at Rösbach south of Mannheim (Küttel et al., 1986) or in LPZ 4 of the Gossau site in Switzerland (Burga, 2006; datings from Geyh and Schlüchter, 1997; Schlüchter et al., 1987; compiled by Preusser et al., 2003) and, under the premise of a climate gradient from west to east, the Charbon IS found at Grande Pile in the Vosges (de Beaulieu and Reille, 1992, datings from Woillard and Mook, 1982) as well. The subsequent LPZ 2 (22.5–22.1 m) with tundra vegetation represents a stadial phase of the penultimate glaciation.

A correlation of the LPZ 3 and 4 (17.9–17.7 and 17.7–17.3 m, respectively) with the following (last) interglacial (Eemian; Schloss, 2012; URG; Schokker et al., 2005; Roer Valley Graben, Netherlands; Zagwijn, 1961; Amersfoort Basin, Netherlands), during the later phase of which boreal forests covered the landscape, can be ruled out because of the total absence of *Abies*. Based on comparisons with long continuous pollen records covering the Eemian and the earlier Late Pleistocene from northeastern France (De Beaulieu and Reille, 1992; Rousseau et al., 2007; Woillard, 1978), the Eifel region (Britzius et al., 2024), and the northern Alpine foreland (e.g. Welten, 1981, 1982; Grüger and Schreiner, 1993; Müller, 2000; Müller et al., 2003), the LPZ 3 and 4 could be assigned to the Odderade IS (MIS 5a, ~75 ka; Behre, 1989;

Stojakowits and Mayr, 2022) due to the lack of *Abies*. This is just in agreement with the results of luminescence dating and suggests that the pollen assemblages reflect a somewhat atypical vegetation composition in the Upper Rhine area due to a strong local signal of the Rhine floodplain. For instance, thermophilous deciduous trees reach during the climatic optimum of the Odderade IS a maximum of >70 % at Grande Pile (Woillard, 1978), up to 30 % at Sulzberg-Baden (Welten, 1981, 1982) and a maximum of 20 % at Füramoos (Müller et al., 2003) reflecting the climate gradient with increasing continentality from west to east. This would explain the fact that the non-arboreal pollen and *Alnus* values, corresponding to the floodplain vegetation, are higher and the amounts of thermophilous tree taxa are lower in our record compared to the above-mentioned pollen profiles from north-eastern France and the Alpine foreland. An assignment of LPZ 3 and 4 to the Brörup IS (MIS 5c, ~90 ka; Stojakowits and Mayr, 2022) would be compatible with the luminescence data but appears unlikely due to the continued findings of *Picea* and *Larix*, while *Abies* is absent. However, the early phase of this IS between the so-called 'Montaigu event' (Reille et al., 1992) and the slight spread of *Abies* cannot be entirely excluded. LPZ 3 and 4 could possibly also be an equivalent of the Dürnten IS described by Welten (1981, 1982), which is characterised by more open boreal forests, composed of pine and spruce with some larch, compared to the preceding Odderade IS. Younger IS of MIS 3 can be ruled out. For instance, the pollen record of a peat layer situated in the Upper Rhine Graben south of Heidelberg, which was correlated with the Hengelo IS (~40 ka; Behre, 1989; Stojakowits and Mayr, 2022) based on radiocarbon dating, revealed an open pine forest with some spruce (<10 %) and probably little larch, too (Küttel et al., 1986). Time-equivalents of the Denekamp IS (~30 ka; Behre, 1989; Stojakowits and Mayr, 2022) just reflect phases with open pine taiga without any occurrence of spruce (e.g. Becker et al., 2006; Duprat-Oualid et al., 2017). In this context, the site of Achenheim is noteworthy as well, as some pollen data exist from its loess sequence (Heim et al., 1984). Unfortunately, the results gained are not suited for comparisons because of low sample resolution and low counted pollen sums.

The number and size of samples for gastropod extraction, collected between ~13 and ~9 m depth (Fig. 3), was very limited. Therefore, the small number of specimens precludes reliable, detailed conclusions regarding palaeoenvironment and eventual biostratigraphic placement. The species encountered are typical of Pleistocene loess sequences, and two of them (*Vitrea crystallina* and *Vertigo genesii*) are only present in the region during the Late Pleistocene Upper Pleniglacial (Moine, 2014). Nevertheless, the observed molluscan assemblages do not help constraining the depositional age, as molluscan faunas from the last and penultimate glacial periods often show similar compositions (see penultimate-glaciation assemblages reported in Limondin-Lozouet and Gauthier, 2003; Rähle, 2004). Noteworthy is the apparent absence of the generally abundant taxon *Pupilla muscorum*, which can however be explained by the small sample sizes (~5 % of the 10-L samples classically taken in loess). All molluscan samples point toward a tundra-like vegetation. Tentatively, sample G1 differs by the presence of a shrubby-environment component with *V. crystallina*, *Arianta arbustorum* and *Columella columella*, and species indicative of ponds (*V. genesii* and cf. *Stagnicola palustris*). With only *V. crystallina*, *Cochlicopa lubrica* and *Pupilla alpicola*, these two components appear to diminish in G2. Normalised to 10 L their abundances would be intermediate between stadial and interstadial ones, whereas those of G3 and G4 would rather fit with stadial conditions. In G3, the sole presence of *A. arbustorum* and *C. columella* suggests a less diversified bushy component and the even weaker richness of G4 suggests a shift to a discontinuous vegetation cover. The molluscan faunas of G2 and G3 are in qualitative agreement with those observed in Late Pleistocene loess sequences at Nussloch (~100 km NE; Moine et al., 2005; 2008), and G1 is compatible with the pollen-based vegetational reconstruction for LPZ 1 and 2.

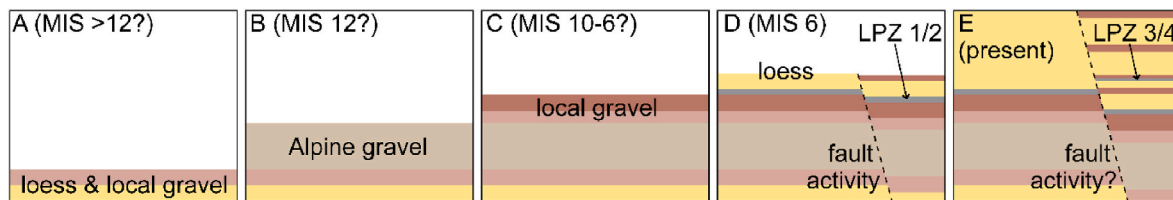


Fig. 6. Sketch of the proposed sequence of depositional events at and around OWI (cf. Figs. 3 and 5).

## 5. Conclusions

A new stratigraphic profile from the central URG near Offenburg (OWI) was introduced and the sequence of depositional events reconstructed, which is summarised on Fig. 6. An older Mid-Pleistocene surface of loess and gravel with locally-derived components, as recovered in a neighbouring borehole (Fig. 6A) was covered by a massive layer of Alpine glaciofluvial outwash, potentially during MIS 12 (Fig. 6B). Deposition of mixed (dated to MIS 8), and lastly purely local gravel followed (Fig. 6C). Starting in MIS 6, the (glacio-)fluvial deposits became overlain by fines. At their base, they contain organic material and an interstadial to stadial pollen sequence (penultimate glaciation; LPZ 1 and 2) compatible with molluscs encountered in core 7513/3409 (sample G1), before transitioning into pure loess deposited in a humid tundra environment first shrubby then discontinuously vegetated. At the same time, subsidence along a fault to the south of OWI is proposed, with the resulting topography being filled in by local-facies gravel (Fig. 6D). Intercalated gravel layers in OWI (and fines with an Early Late Pleistocene pollen sequence, LPZ 3 and 4) suggest that the same fault was episodically active until present day (Fig. 6E).

This study highlights the relevance of the sedimentary record that is stored, but still mostly untapped, in large parts of the URG. Due to its subsidence history, the graben has provided accommodation space for remarkably continuous deposition throughout – but not limited to – the Quaternary. In comparison, phases of nondeposition and/or erosion were brief, and therefore the corresponding sediments preserved valuable information on the long-term climatic evolution of central Europe, its impact on floras and faunas, past glaciations of the Alpine headwaters, and of the graben's neotectonic history itself. Thus, there is ample potential for further research uncovering new, and linking existing, puzzle pieces of the URG's depositional record.

## CRediT authorship contribution statement

**Lukas Gegg:** Writing – review & editing, Writing – original draft, Visualization, Validation, Project administration, Methodology, Investigation, Formal analysis, Data curation, Conceptualization. **Olivier Moine:** Writing – review & editing, Validation, Methodology, Investigation, Formal analysis. **Philipp Stojakowits:** Writing – review & editing, Validation, Methodology, Investigation, Formal analysis. **Frank Preusser:** Writing – review & editing, Validation, Methodology, Investigation, Formal analysis.

## Funding

This research did not receive a specific grant from funding agencies in the public, commercial, or not-for-profit sectors. Preparation of pollen samples was supported by Wissenschaftliche Gesellschaft Freiburg im Breisgau.

## Declaration of competing interest

The authors declare that they have no known competing financial interests or personal relationships that could have appeared to influence the work reported in this paper.

## Acknowledgements

We thank the Geological State Survey of Baden-Württemberg (LGRB), notably Ulrike Wielandt-Schuster, for valuable recommendations, and Deutsche Bahn and gbm Gesellschaft für Baugologie und -meßtechnik for providing access to the drill cores. Nicole Jentz and Oscar Petrou supported sampling and gravel petrographic analyses. Laura Jacob extracted gastropod shells, while loss-on-ignition measurements and sample preparation for luminescence dating were done by Margarita Nuss. Pollen samples were prepared by Anna Schubert ([www.pollenanalyse-berlin-brandenburg.de](http://www.pollenanalyse-berlin-brandenburg.de)) with financial support of Wissenschaftliche Gesellschaft Freiburg im Breisgau. We thank also editor Neil Glasser and an anonymous reviewer for constructive recommendations.

## Data availability

Data will be made available on request.

## References

- Antoine, P., Rousseau, D.-D., Moine, O., Kunesch, S., Hatté, C., Lang, A., Tissoux, H., Zöller, L., 2009. Rapid and cyclic aeolian deposition during the Last Glacial in European loess: a high-resolution record from Nussloch, Germany. *Quat. Sci. Rev.* 28, 2955–2973. <https://doi.org/10.1016/j.quascirev.2009.08.001>.
- Bank, R.A., Bieler, R., Bouchet, P., Decock, W., Dekeyser, S., Kroh, A., Marshall, B., Neubauer, T.A., Neubert, E., Rosenberg, G., Sartori, A.F., Schneider, S., Trias-Verbeek, A., Vandepitte, L., Vanhoorne, B., Gofas, S., 2014. MolluscaBase – announcing a world register of all molluscs. Presented at the 7th Congress of the European Malacological Societies.
- Barth, A., Ritter, J., Wenzel, F., 2015. Spatial variations of earthquake occurrence and coseismic deformation in the upper rhine graben, central europe. *Tectonophysics* 651, 172–185.
- Bartz, J., 1982. Quartär und Jungtertiär II im Oberrheingraben im Großraum Karlsruhe mit Beiträgen von Brellie, G. von der & Maus, H. *Geol. Jahrb. A* 63, 3–237.
- Becker, A., Ammann, B., Anselmetti, F.S., Hirt, A.M., Magny, M., Millet, L., Rachoud, A.-M., Sampietro, G., Wüthrich, C., 2006. Paleoenvironmental studies on lake bergsee, Black forest, Germany. *Neues Jahrbuch Geol. Palaontol. Abhand.* 405–445. <https://doi.org/10.1127/njgpa/240/2006/405>.
- Behre, K.-E., 1989. Biostratigraphy of the last glacial period in Europe. *Quat. Sci. Rev.* 8, 25–44. [https://doi.org/10.1016/0277-3791\(89\)90019-X](https://doi.org/10.1016/0277-3791(89)90019-X).
- Bellier, O., Cushing, E.M., Sébrier, M., 2021. Thirty years of paleoseismic research in metropolitan France. *C. R. Geosci.* 353, 339–380.
- Beug, H.J., 2004. Leitfaden der Pollenbestimmung für Mitteleuropa und angrenzende Gebiete. Verlag Dr. Friedrich Pfeil, Munich.
- Bludau, W., Groschopf, R., Schreiner, A., 1994. Ein Riß-Interstadial bei Riedmatt am Hochrhein. *Jahresber. Mittl. Oberrheinischen Geol. Vereins* 295–324. <https://doi.org/10.1127/jmogv/76/1994/295>.
- Boenigk, W., 1987. Petrographische Untersuchungen jungtertiärer und quartärer Sedimente am linken Oberrhein. *Jahresberichte und Mitteilungen des oberrheinischen geologischen Vereins*, pp. 357–394.
- Britzius, S., Dreher, F., Maisel, P., Sirocko, F., 2024. Vegetation patterns during the last 132,000 Years: a synthesis from twelve Eifel maar sediment cores (Germany): the ELSA-23-pollen-stack. *Quaternary* 7, 8.
- Brost, E., Ellwanger, D., Bludau, W., Rolf, C., 1991. Einige Ergebnisse neuerer geoelektrischer und stratigraphischer Untersuchungen im Gebiet zwischen Kaiserstuhl und Kehl. *Geol. Jahrbuch Reihe E Geophys.* 71–81.
- Buechi, M.W., Graf, H.R., Haldimann, P., Lowick, S.E., Anselmetti, F.S., 2018. Multiple Quaternary erosion and infill cycles in overdeepened basins of the northern Alpine foreland. *Swiss J. Geosci.* 111, 1–34. <https://doi.org/10.1007/s00015-017-0289-9>.
- Buechi, M.W., Landgraf, A., Madritsch, H., Mueller, D., Knipping, M., Nyffenegger, F., Preusser, F., Schaller, S., Schnellmann, M., Deplazes, G., 2024. Terminal glacial overdeepenings: patterns of erosion, infilling and new constraints on the glaciation history of Northern Switzerland. *Quat. Sci. Rev.* 344, 108970. <https://doi.org/10.1016/j.quascirev.2024.108970>.

- Buraczynski, J., Butrym, J., 1984. La datation des loess du profil d'Achenheim (Alsace) à l'aide de la méthode de thermoluminescence. *Quaternaire* 21, 201–209.
- Burga, C.A., 2006. Zum Mittelwürm des Zürcher Oberlandes am Beispiel des Schieferkohle Profiles von Gossau (Kanton Zürich). *Vierteljahrsschrift der Naturforschenden Gesellschaft Zürich* 151, 91–100.
- Claude, A., Akçar, N., Ivy-Ochs, S., Schlunegger, F., Rentzel, P., Pümpin, C., Tikhomirov, D., Kubik, P.W., Vockenhuber, C., Dehnert, A., 2017. Chronology of quaternary terrace deposits at the locality hohle gasse (Pratteln, NW Switzerland). *Swiss J. Geosci.* 110, 793–809. <https://doi.org/10.1007/s00015-017-0278-z>.
- De Beaulieu, J.-L., Reille, M., 1992. The last climatic cycle at La Grande Pile (Vosges, France) a new pollen profile. *Quat. Sci. Rev.* 11, 431–438.
- Degering, D., Degering, A., 2020. Change is the only constant - time-dependent dose rates in luminescence dating. *Quat. Geochronol.* 58, 101074. <https://doi.org/10.1016/j.quageo.2020.101074>.
- Dèzes, P., Schmid, S.M., Ziegler, P.A., 2004. Evolution of the European Cenozoic Rift System: interaction of the alpine and pyrenean orogens with their foreland lithosphere. *Tectonophysics* 389, 1–33. <https://doi.org/10.1016/j.tecto.2004.06.011>.
- Duprat-Oualid, F., Riüs, D., Bégeot, C., Magny, M., Millet, L., Wulf, S., Appelt, O., 2017. Vegetation response to abrupt climate changes in Western Europe from 45 to 14.7k cal a BP: the Bergsee lacustrine record (Black Forest, Germany). *J. Quat. Sci.* 32, 1008–1021. <https://doi.org/10.1002/jqs.2972>.
- Ellwanger, D., 2011. Ortenau-Formation. *LithoLex*. <https://litholex.bgr.de>.
- Ellwanger, D., Franz, M., Wielandt-Schuster, U., 2012. Zur einföhrung: heidelberg becken, oberschwaben-oberrhein, geosystem rhein. *LGRB-Informationen* 26, 7–24.
- Ellwanger, D., Gabriel, G., Simon, T., Wielandt-Schuster, U., Greiling, R.O., Hagedorn, E.-M., Hahne, J., Heinz, J., 2009. Long sequence of quaternary rocks in the Heidelberg Basin depocentre. *E&G Quat. Sci. J.* 57 (3), 316–337. <https://doi.org/10.3285/eg.57.3-4>.
- Ellwanger, D., Wielandt-Schuster, U., Franz, M., Simon, T., 2011. The quaternary of the southwest German alpine foreland (Bodensee-Oberschwaben, Baden-Württemberg, southwest Germany). *E&G J. Quat. Sci.* 60, 306–328. <https://doi.org/10.3285/eg.60.2-3.07>.
- Fægri, K., Iversen, J., 1989. *Textbook of Pollen Analysis*, fourth ed. John Wiley & Sons Ltd.
- Frechen, M., Schweitzer, U., Zander, A., 1996. Improvements in sample preparation for the fine grain technique. *Ancient TL* 14, 15–17.
- Gabriel, G., Ellwanger, D., Hoselmann, C., Weidenfeller, M., Wielandt-Schuster, U., The Heidelberg Basin Project Team, 2013. The Heidelberg Basin, Upper Rhine Graben (Germany): a unique archive of quaternary sediments in central Europe. *Quat. Int.* 292, 43–58. <https://doi.org/10.1016/j.quaint.2012.10.044>.
- Gegg, L., Anselmetti, F.S., Deplazes, G., Knipping, M., Madritsch, H., Mueller, D., Preusser, F., Vogel, H., Buechi, M.W., 2023. Rinikerfeld Palaeolake (Northern Switzerland) – a sedimentary archive of landscape and climate change during the penultimate glacial cycle. *J. Quat. Sci.* 38, 174–185. <https://doi.org/10.1002/jqs.3471>.
- Gegg, L., Griebeling, F.A., Jentz, N., Wielandt-Schuster, U., 2024a. Towards a quantitative lithostratigraphy of Pleistocene fluvial deposits in the southern Upper Rhine Graben. *E&G J. Quat. Sci.* 73, 239–249.
- Gegg, L., Jacob, L., Moine, O., Nelson, E., Penkman, K.E.H., Schwahn, F., Stojakowits, P., White, D., Wielandt-Schuster, U., Preusser, F., 2024b. Climatic and tectonic controls on deposition in the Heidelberg Basin, Upper Rhine Graben, Germany. *Quat. Sci. Rev.* 345, 109018. <https://doi.org/10.1016/j.quascirev.2024.109018>.
- GeORG-Projektteam, 2013. *Geopotenziale des tieferen Untergrundes im Oberrheingraben, Fachlich-Technischer Abschlussbericht des INTERREG-Projekts GeORG, Teil 1: Zusammenfassung, LGRB Informationen*.
- Geyh, M.A., Schlüchter, C., 1997. Calibration of the 14C time scale beyond 22,000 BP. *Radiocarbon* 40, 475–482.
- Graf, H.R., 2009. Stratigraphie und Morphogenese von frühpleistozänen Ablagerungen zwischen Bodensee und Klettgau. *E&G J. Quat. Sci.* 58, 12–53. <https://doi.org/10.3285/eg.58.1.02>.
- Grüger, E., Schreiner, A., 1993. Riß/Würm- und würmzeitliche Ablagerungen im Wurzach Becken (Rheingletschergebiet). *Neues Jahrbuch Geol. Palaontol. Abhand.* 81–117. <https://doi.org/10.1127/njgpa/189/1993/81>.
- Hagedorn, E.M., Boenigk, W., 2008. The Pliocene and Quaternary sedimentary and fluvial history in the Upper Rhine Graben based on heavy mineral analyses. *Neth. J. Geosci. Geol. Mijnbouw* 87, 21–32. <https://doi.org/10.1017/S001677460002401X>.
- Heim, J., Lautridou, J., Maucorps, J., Puisségur, J., Rousseau, D., Sommé, J., Thévenin, A., Van Vliet-Lanoé, B., 1984. Achenheim: Loess et formations fluviales quaternaires d'Alsace. *INQUA Subcommittee of European Quaternary Stratigraphy. Livret-guide* 13, 4–14.
- Heiri, O., Lotter, A.F., Lemcke, G., 2001. Loss on ignition as a method for estimating organic and carbonate content in sediments: reproducibility and comparability of results. *J. Paleolimnol.* 25, 101–110. <https://doi.org/10.1023/A:1008119611481>.
- Hoselmann, C., 2009. The Pliocene and Pleistocene fluvial evolution in the northern Upper Rhine Graben based on results of the research borehole at Viernheim (Hessen, Germany). *E&G Quat. Sci. J.* 57 (2), 286–314. <https://doi.org/10.3285/eg.57.3-4>.
- Kock, S., Huggenberger, P., Preusser, F., Rentzel, P., Wetzel, A., 2009. Formation and evolution of the lower terrace of the Rhine River in the area of Basel. *Swiss J. Geosci.* 102, 307–321. <https://doi.org/10.1007/s00015-009-1325-1>.
- Köbel, L., Köbel, T., Herrmann, L., Kaymakci, E., Ghergut, I., Poirel, A., Schneider, J., 2023. Lithium extraction from geothermal brines in the Upper Rhine Graben: a case study of potential and current state of the art. *Hydrometallurgy* 221, 106131. <https://doi.org/10.1016/j.hydromet.2023.106131>.
- Küttel, M., Löscher, M., Hölzer, A., 1986. Ergebnisse paläobotanischer Untersuchungen zur Stratigraphie und Ökologie des Wurms im Oberrheingraben zwischen Karlsruhe und Mannheim. *E&G J. Quat. Sci.* 36, 75–88. <https://doi.org/10.3285/eg.36.1.06>.
- Lambert, J., Winter, T., Dewez, T.J.B., Sabourault, P., 2005. New hypotheses on the maximum damage area of the 1356 Basel earthquake (Switzerland). *Quat. Sci. Rev.* 24, 381–399. <https://doi.org/10.1016/j.quascirev.2004.02.019>.
- Lang, S., Hornung, J.M.K., Ruckwied, K., Hoppe, A., 2011. Tektonik und Sedimentation am Rand des Oberrheingrabens in Darmstadt im Mittel- und Oberpleistozän. *Geol. Jahrb. Hessen* 137, 19–53.
- Lauer, T., Frechen, M., Hoselmann, C., Tsukamoto, S., 2010. Fluvial aggradation phases in the Upper Rhine Graben — new insights by quartz OSL dating. *PGA (Proc. Geol. Assoc.)* 121, 154–161. <https://doi.org/10.1016/j.pgeola.2009.10.006>.
- Lehmkuhl, F., Nett, J.J., Pötter, S., Schulte, P., Sprafke, T., Jary, Z., Antoine, P., Wacha, L., Wolf, D., Zerboni, A., Hošek, J., Marković, S.B., Obrecht, I., Sümeji, P., Veres, D., Zeeden, C., Boemke, B., Schaubert, V., Viehweger, J., Hambach, U., 2021. Loess landscapes of Europe – mapping, geomorphology, and zonal differentiation. *Earth Sci. Rev.* 215, 103496. <https://doi.org/10.1016/j.earscirev.2020.103496>.
- Lemeille, F., Cushing, M.E., Cotton, F., Grellet, B., Ménillet, F., Audry, J.-C., Renardy, F., Fléhoc, C., 1999. Traces d'activité pléistocène de failles dans le Nord du fossé du Rhin supérieur (plaine d'Alsace, France). *Comptes Rendus Acad. Sci. - Ser. IIA Earth Planet. Sci.* 328, 839–846.
- LGRB, 2023. Geologische Karte von Baden-Württemberg 1:50.000 (GeoLa). via. <https://maps.lgrb-bw.de/>.
- Li, B., Li, S.-H., 2011. Luminescence dating of K-feldspar from sediments: a protocol without anomalous fading correction. *Quat. Geochronol.* 6, 468–479. <https://doi.org/10.1016/j.quageo.2011.05.001>.
- Limondin-Lozouet, N., Gauthier, A., 2003. Biocénoses Pléistocènes des séquences loessiques de Villier-Adam (Val d'Oise, France); Etudes Malacologiques et palynologiques. *Quaternaire* 14, 237–252.
- Lisiecki, L.E., Raymo, M.E., 2005. A Pliocene-Pleistocene stack of 57 globally distributed benthic  $\delta^{18}O$  records. *Paleoceanography* 20. <https://doi.org/10.1029/2004PA001071>.
- Ložek, V., 1964. Quartärmollusken der Tschechoslowakei, *Rozprawy Ústředního ústavu geologického*. Prague.
- Marik, M., Serra, E., Gegg, L., Wölki, D., Preusser, F., 2024. Combined different luminescence dating approaches on fluvial gravel deposits from the southern Upper Rhine Graben. *Quat. Geochronol.* 82, 101536. <https://doi.org/10.1016/j.quageo.2024.101536>.
- Menzies, J., Ellwanger, D., 2015. Climate and paleo-environmental change within the Mannheim Formation near Heidelberg, Upper Rhine Valley, Germany: a case study based upon microsedimentological analyses. *Quat. Int.* 386, 137–147. <https://doi.org/10.1016/j.quaint.2015.03.037>.
- Moine, O., 2014. Weichselian Upper Pleniglacial environmental variability in north-western Europe reconstructed from terrestrial mollusc faunas and its relationship with the presence/absence of human settlements. *Quat. Int.* 337, 90–113. <https://doi.org/10.1016/j.quaint.2014.02.030>.
- Moine, O., Rousseau, D.-D., Antoine, P., 2008. The impact of Dansgaard-Oeschger cycles on the loessic environment and malacofauna of Nussloch (Germany) during the Upper Weichselian. *Quat. Res.* 70, 91–104.
- Moine, O., Rousseau, D.-D., Antoine, P., 2005. Terrestrial mollusc records of Weichselian Lower to Middle Pleniglacial climatic changes from the Nussloch loess series (Rhine Valley, Germany): the impact of local factors. *Boreas* 34, 363–380. <https://doi.org/10.1111/j.1502-3885.2005.tb01107.x>.
- Montenat, C., Barrier, P., Hibsich, C., others, 2007. Seismites: an attempt at critical analysis and classification. *Sediment. Geol.* 196, 5–30.
- Müller, U.C., 2000. A Late-Pleistocene pollen sequence from the Jammertal, south-western Germany with particular reference to location and altitude as factors determining Eemian forest composition. *Veg. Hist. Archaeobotany* 9, 125–131. <https://doi.org/10.1007/BF01300062>.
- Müller, U.C., Pross, J., Bibus, E., 2003. Vegetation response to rapid climate change in central Europe during the past 140,000 yr based on evidence from the Fürmoos pollen record. *Quat. Res.* 59, 235–245. [https://doi.org/10.1016/S0033-5894\(03\)00005-X](https://doi.org/10.1016/S0033-5894(03)00005-X).
- Murray, A.S., Olley, J.M., Caitcheon, G.G., 1995. Measurement of equivalent doses in quartz from contemporary water-lain sediments using optically stimulated luminescence. *Quat. Sci. Rev.* 14, 365–371. [https://doi.org/10.1016/0277-3791\(95\)00030-5](https://doi.org/10.1016/0277-3791(95)00030-5).
- Nivière, B., Bruestle, A., Bertrand, G., Carretier, S., Behrmann, J., Gourry, J.-C., 2008. Active tectonics of the southeastern upper rhine graben, Freiburg area (Germany). *Quat. Sci. Rev.* 27, 541–555. <https://doi.org/10.1016/j.quascirev.2007.11.018>.
- Pena-Castellnou, S., Hürtgen, J., Baize, S., Jomard, H., Cushing, E.M., Abbas, W., Reichert, K., 2025. Active faulting of the southern segment of the Rhine River Fault, southern Germany: geomorphological and paleoseismological evidence. *Quat. Int.* 716, 109589. <https://doi.org/10.1016/j.quaint.2024.11.007>.
- Pena-Castellnou, S., Hürtgen, J., Baize, S., Preusser, F., Mueller, D., Jomard, H., Cushing, E.M., Rockwell, T.K., Seitz, G., Cinti, F.R., Ritter, J., Reichert, K., 2023. Surface rupturing earthquakes along the eastern rhine graben boundary fault near ettlingen-oberweier (Germany). *Tectonophysics* 869, 230114. <https://doi.org/10.1016/j.tecto.2023.230114>.
- Peters, G., Van Balen, R.T., 2007a. Tectonic geomorphology of the northern upper rhine graben, Germany. *Global Planet. Change* 58, 310–334. <https://doi.org/10.1016/j.gloplacha.2006.11.041>.

- Peters, G., Van Balen, R.T., 2007b. Pleistocene tectonics inferred from fluvial terraces of the northern Upper Rhine Graben, Germany. *Tectonophysics* 430, 41–65. <https://doi.org/10.1016/j.tecto.2006.10.008>.
- Pigati, J.S., McGeehin, J.P., Muhs, D.R., Bettis, E.A., 2013. Radiocarbon dating late Quaternary loess deposits using small terrestrial gastropod shells. *Quat. Sci. Rev.* 76, 114–128. <https://doi.org/10.1016/j.quascirev.2013.05.013>.
- Preusser, F., Büschelberger, M., Kemna, H.A., Miocic, J., Mueller, D., May, J.-H., 2021. Exploring possible links between Quaternary aggradation in the Upper Rhine Graben and the glaciation history of northern Switzerland. *Int. J. Earth Sci.* 110, 1827–1846. <https://doi.org/10.1007/s00531-021-02043-7>.
- Preusser, F., Degering, D., Fülling, A., Miocic, J., 2023. Complex dose rate calculations in luminescence dating of lacustrine and palustrine sediments from niederweningen, northern Switzerland. *Geochronometria* 50, 28–49. <https://doi.org/10.2478/geochr-2023-0003>.
- Preusser, F., Geyh, M.A., Schlichter, C., 2003. Timing of Late Pleistocene climate change in lowland Switzerland. *Quat. Sci. Rev.* 22, 1435–1445.
- Preusser, F., Graf, H.R., Keller, O., Krayss, E., Schlichter, C., 2011. Quaternary glaciation history of northern Switzerland. *E&G J. Quat. Sci.* 60, 282–305. <https://doi.org/10.1016/j.quaint.2012.08.1202>.
- Preusser, F., May, J.-H., Eschbach, D., Trauerstein, M., Schmitt, L., 2016. Infrared stimulated luminescence dating of 19th century fluvial deposits from the upper Rhine River. *Geochronometria* 43, 131–142. <https://doi.org/10.1515/geochr-2015-0045>.
- Puisségur, J.-J.A., 1976. Mollusques continentaux quaternaires de Bourgogne. Significations stratigraphiques et climatiques. Rapports avec d'autres faunes boréales en France, Mémoires géologiques de l'Université de Dijon. Doin, Paris.
- Rähle, W., 2005. Eine mittelpleistozäne Molluskenfauna aus dem Oberen Zwischenhorizont des nördlichen Oberrheingrabens (Bohrung Mannheim-Lindenhof). *Mainz. Geowiss. Mitt.* 33, 9–20.
- Rähle, W., 2004. Mollusken aus zwei bedeutenden mittel- und jungpleistozänen Lößprofilen des mittleren Neckarraumes (Baden-Württemberg) und ihre ökologisch-stratigraphische Aussage. *Tübinger Geowiss. Arb. Reihe D* 10, 219–240.
- Reille, M., 1998. Pollen et spores d'Europe et d'Afrique du Nord. *Laboratoire de Botanique historique et Palynologie, Marseille*.
- Reille, M., Guiot, J., de Beaulieu, J.-L., 1992. The Montagu Event: an abrupt climatic change during the early Würm in Europe. In: *Start of a Glacial*. Springer, pp. 85–95.
- Richter, D., Richter, A., Dornich, K., 2013. Lexsyg — a new system for luminescence research. *Geochron* 40, 220–228. <https://doi.org/10.2478/s13386-013-0110-0>.
- Richter, D., Woda, C., Dornich, K., 2020. A new quartz for  $\gamma$ -transfer calibration of radiation sources. *Geochronometria* 47, 23–34. <https://doi.org/10.2478/geochr-2020-0020>.
- Rousseau, D.-D., Hatté, C., Duzer, D., Schevin, P., Kukla, G., Guiot, J., 2007. Estimates of temperature and precipitation variations during the Eemian interglacial: new data from the grande pile record (GP XXI). In: *Developments in Quaternary Sciences*. Elsevier, pp. 231–238.
- Scheidt, S., Hambach, U., Rolf, C., 2015. A consistent magnetic polarity stratigraphy of late Neogene to Quaternary fluvial sediments from the Heidelberg Basin (Germany): a new time frame for the Plio-Pleistocene palaeoclimatic evolution of the Rhine Basin. *Global Planet. Change* 127, 103–116. <https://doi.org/10.1016/j.gloplacha.2015.01.004>.
- Schloss, S., 2012. Ein Eem-zeitliches Pollenprofil aus der Nördlichen Oberrheinniederung bei Philippsburg. *LGRB Informationen* 26, 155–162.
- Schlichter, C., Akçar, N., Ivy-Ochs, S., 2021. The quaternary period in Switzerland. In: *Landscapes and Landforms of Switzerland*. Springer, pp. 47–69.
- Schlichter, C., Maisch, M., Suter, J., Fitze, P., Keller, W.A., Burga, C.A., Wynistorf, E., 1987. Das Schieferkohlen-Profil von Gossau (Kanton Zürich) und seine stratigraphische Stellung innerhalb der letzten Eiszeit. *Vierteljahrsschrift der Naturforschenden Gesellschaft Zürich* 132, 135–174.
- Schokker, J., Cleveringa, P., Murray, A.S., Wallinga, J., Westerhoff, W.E., 2005. An OSL dated middle and late quaternary sedimentary record in the Roer Valley Graben (southeastern Netherlands). *Quat. Sci. Rev.* 24, 2243–2264. <https://doi.org/10.1016/j.quascirev.2005.01.010>.
- Schulze, T., Schwahn, L., Fülling, A., Zeeden, C., Preusser, F., Sprafke, T., 2022. Investigating the loess–palaeosol sequence of Bahlingen-Schönenberg (Kaiserstuhl), southwestern Germany, using a multi-methodological approach. *E&G J. Quat. Sci.* 71, 145–162. <https://doi.org/10.5194/egqsj-71-145-2022>.
- Schumacher, M.E., 2002. Upper Rhine Graben: role of preexisting structures during rift evolution. *Tectonics* 21. <https://doi.org/10.1029/2001TC900022>.
- Schwahn, L., Schulze, T., Fülling, A., Zeeden, C., Preusser, F., Sprafke, T., 2023. Multi-method study of the Middle Pleistocene loess–palaeosol sequence of Köndringen, SW Germany. *E&G Quat. Sci. J.* 72, 1–21. <https://doi.org/10.5194/egqsj-72-1-2023>.
- Shipton, Z.K., Meghraoui, M., Monro, L., 2017. Seismic Slip on the West Flank of the Upper Rhine Graben (France–Germany): Evidence from Tectonic Morphology and Cataclastic Deformation Bands, vol. 432. Geological Society, London, Special Publications, pp. 147–161.
- Simon, T., Seyfried, H., 2020. Eine frühholozäne oberflächenbrechende Verwerfung im Raum Karlsruhe. *Jahresber. Mittl. Oberrheinischen Geol. Vereins* 363–378.
- Stober, I., Jägle, M., Kohl, T., 2023. Optimizing scenarios of a deep geothermal aquifer storage in the southern Upper Rhine Graben. *Geotherm. Energy* 11, 34. <https://doi.org/10.1186/s40517-023-00275-1>.
- Stojakowits, P., Mayr, C., 2022. Chapter three - quaternary palynostratigraphy of Germany with special emphasis on the late Pleistocene. In: Montanari, M. (Ed.), *Stratigraphy & Timescales, Integrated Quaternary Stratigraphy*. Academic Press, pp. 81–136. <https://doi.org/10.1016/bs.sats.2022.09.001>.
- Weidenfeller, M., Kärcher, T., 2008. Tectonic influence on fluvial preservation: aspects of the architecture of Middle and Late Pleistocene sediments in the northern Upper Rhine Graben, Germany. *Neth. J. Geosci.* 87, 33–40. <https://doi.org/10.1017/S0016774600024021>.
- Weidenfeller, M., Knipping, M., 2009. Correlation of Pleistocene sediments from boreholes in the ludwigshafen area, western Heidelberg Basin. *E&G J. Quat. Sci.* 57 (1), 270–285. <https://doi.org/10.3285/eg.57.3-4>.
- Welten, M., 1982. Pollenanalytische Untersuchungen im Jüngeren Quartär des nördlichen Alpenvorlandes der Schweiz. Schweizerische Geologische Kommission, Stämpfli + Cie AG, Bern.
- Welten, M., 1981. Verdrängung und Vernichtung der anspruchsvollen Gehölze am Beginn der letzten Eiszeit und die Korrelation der Frühwürm-Interstadiale in Mittel- und Nordeuropa. *E&G J. Quat. Sci.* 31, 187–202. <https://doi.org/10.3285/eg.31.1.14>.
- Welter-Schultes, F.W. (Ed.), 2012. *European non-marine molluscs: a guide for species identification = Bestimmungsbuch für europäische Land- und Süßwassermollusken*, 1. ed. ed. Planet Poster Ed. Göttingen.
- Wirsing, G., Luz, A., 2007. *Hydrogeologischer Bau und Aquifereigenschaften der Lockergesteine im Oberrheingraben (Baden-Württemberg)*, vol. 19. LGRB Informationen.
- Woillard, G.M., 1978. Grande Pile peat bog: a continuous pollen record for the last 140,000 years. *Quat. Res.* 9, 1–21.
- Woillard, G.M., Mook, W.G., 1982. Carbon-14 dates at Grande Pile: correlation of land and sea chronologies. *Science* 215 (4529), 159–161.
- Zagwijn, W.H., 1961. Vegetation, climate and radiocarbon datings in the late Pleistocene of The Netherlands, Part I: eemian and early weichselian. *Medede. Geol. Sticht. N. S.* 14, 15–45.
- Ziegler, P.A., 1992. European Cenozoic rift system. *Tectonophysics* 208, 91–111. [https://doi.org/10.1016/0040-1951\(92\)90338-7](https://doi.org/10.1016/0040-1951(92)90338-7).